DOI: 10.1002/ejoc.200800191

Redox-Controlled Fluorescence Modulation in a BODIPY-Quinone Dyad

Andrew C. Benniston,*[a] Graeme Copley,[a] Kristopher J. Elliott,[a] Ross W. Harrington,[b] and William Clegg[b]

Keywords: BODIPY / Fluorescence / Molecular devices / Redox chemistry / Sensors

The synthesis and properties of two closely related boron dipyrromethene (BODIPY) derived dyads, incorporating redox-active quinone units appended at the *meso* position, are described. For one dyad, the quinone unit is attached directly to the BODIPY core, whereas a phenylene spacer separates the two units in the second compound. Each of the quinone units is readily converted, by both chemical and electrochemical means, to the corresponding hydroquinone derivative. The strong fluorescence normally associated with the BODIPY unit is efficiently quenched in both dyads in their quinone forms. This is attributed to deactivation of the first excited singlet state by a way of an intramolecular electron-transfer process. By comparison, moderately intense fluorescence is observed for the hydroquinone derivative containing the phenylene spacer, but not for the analogous directly coupled dyad.

The potential sensing capabilities of the phenylene-spaced BODIPY quinone and hydroquinone dyads, towards reducing and oxidising species such as ascorbate and peroxide, were tested in a biomembrane mimic. A reversible modulation in fluorescence could be readily detected by eye under standard UV-light excitation.

Introduction

Interest in the development of innovative probes for monitoring real-time events in micro- to nano-scale environments has grown rapidly over the past decade.[1] This can be traced, in part, to the need for reliable information on physical and/or chemical events occurring in reaction volumes that are extremely difficult to access by conventional imaging technology. In specific cases, the capability to construct miniaturised tools (e.g., nano-electrodes)[2] has opened up new means by which to monitor in situ growth of insoluble residues,[3] corrosion,[4] leakage[5] and flow dynamics,[6] for example. Although we seem certain to witness a great expansion in such technology, the accompanying problem of being able to access ever-smaller dimensions must not be overlooked. Molecular-scale probes,[7] simply by virtue of their size, have the advantage of being able to enter most cavities, pores and cages but need to be equipped with an appropriate signalling system.

Luminescence, in its many disparate forms and including delayed fluorescence,[8] is generally accepted as being a superior signalling method. Indeed, fluorescence can often be observed by the human eye, even for nanomolar concentrations of luminophore, while single-molecule detection can be observed under certain conditions.[9] A general problem inherent to all luminescent sensors is background noise created by other endogenous luminophores that are accidentally excited; time-gated methods using long-lived emitters[10] or delayed emission[11] offer potential solutions to this predicament. The next problem is to provide a failsafe means by which the emission intensity can be related to the property under investigation. This usually requires equipping the fluorophore with ancillary groups that undergo complexation,[12] redox switching[13] or conformational exchange[14] and thereby provide the essential on-off signal. This procedure can be adapted to design fluorescent sensors to monitor, for example, local pH,[15] concentrations of analytes (e.g., Na^+, PO_4^{3-}),[16] drug metabolite products,[17] toxins,[18] nerve agents[19] and reactive oxygen species (ROS).[20a,20b]

The detection of ROS is a field of great topical interest, especially in biomedicine, because they have both beneficial (e.g., smooth muscle relaxation) and harmful (e.g., premature aging) roles.[21] To this end, fluorescent probes for the in situ detection of biological activity have been used widely. A common theme for the mode of action of such probes requires reaction of the ROS to alter the structure of the fluorophore, indirectly converting it from non-luminescent to strongly emissive.[21] Under these conditions, the structural change may be irreversible, such that the probe is effectively redundant after detection. In an endeavour to develop more re-usable redox-responsive fluorescent

[a] Molecular Photonics Laboratory, School of Natural Sciences, Newcastle University,
Newcastle upon Tyne, NE1 7RU, UK
Fax: +44-191 222 6929
E-mail: a.c.benniston@ncl.ac.uk
[b] Crystallography Laboratory, School of Natural Sciences, Newcastle University,
Newcastle upon Tyne, NE1 7RU, UK

Supporting information for this article is available on the WWW under http://www.eurjoc.org/ or from the author.

probes, we have focussed on using the reversible quinone/hydroquinone couple. This redox pair has been used previously with ruthenium(II) (polypyridyl) luminophores as the reporting units,[22a,22b] but such systems have serious disadvantages; most notably, the emission quantum yields are rather low under ambient conditions and highly dependent on temperature while the compounds dissolve only in polar media. To overcome these problems, our attention has turned to the difluoro borondipyrromethene (BODIPY) dyes because these exhibit intense fluorescence in the visible region and undergo reductive/oxidative quenching.[23a,23b] The design element demands that the quinone quenches fluorescence from the BODIPY, due to electron transfer, but conversion to the corresponding hydroquinone restores the emission. A well known issue in this type of sensor concerns how well intramolecular electron transfer competes with the normal radiative process because this competition sets the on-off level. This is not a real problem with long-lived phosphorescence from transition-metal chelates[24] but becomes a serious concern with short-lived organic fluorophores. To allow for this point, we consider two prototypes that differ according to the linkage between the dye and the quencher. The first system has the quinone/hydroquinone unit attached directly to the BODIPY core while the alternative sensor has a phenylene spacer inserted between the terminal groups. The two systems show quite disparate behaviour. The dyads with the spacer show excellent on/off attenuation in fluorescence, and attention is given to both electrochemical and chemical switching. In particular, the systems display the capability to act as reporters for biologically relevant species in a membrane mimic.

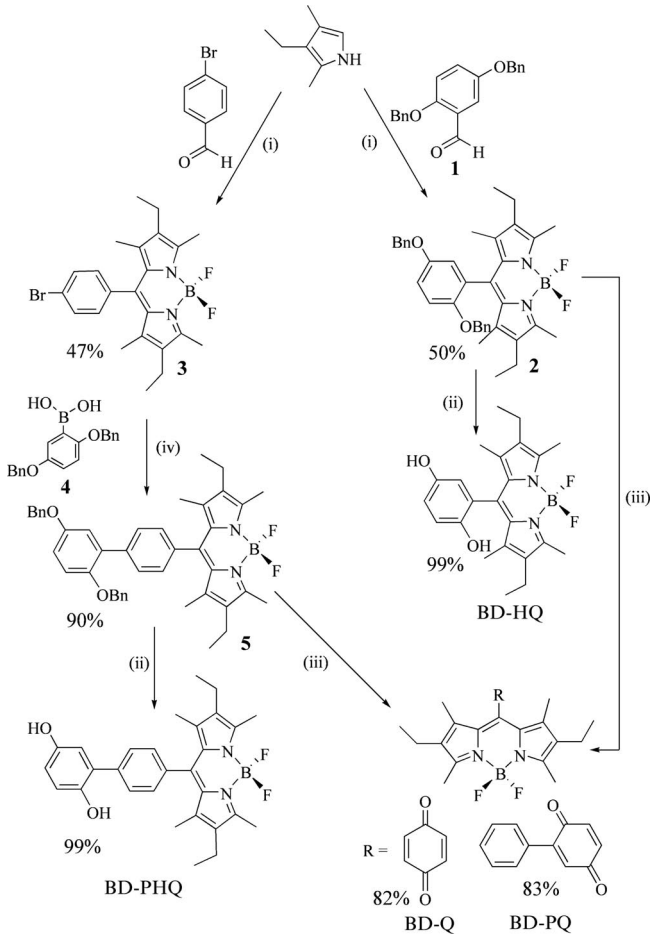

Scheme 1. Reagents and conditions. (i) DCM, TFA, room temp.; DDQ; *N*,*N*-diisopropylethylamine, $BF_3{\cdot}Et_2O$. (ii) H_2, 4 atm, DCM/MeOH, Pd/C (10%). (iii) H_2, 4 atm, DCM/MeOH, Pd/C (10%); DDQ, THF.

Results and Discussion

Synthesis

The synthetic procedures employed to obtain the desired dyads are outlined in Scheme 1 and rely heavily on the tried and tested methods used for the synthesis of other BODIPY derivatives.[25] For preparation of both dyads, the hydroquinone unit was protected as the benzyl ether rather than the corresponding methyl ether, because of ease of removal. In fact, our first synthetic strategy did produce the methoxy versions (BD-M, BD-PM), but deprotection (BBr_3) resulted in very low yields of the final products. These two compounds, however, are useful as controls for subsequent electrochemical and photophysical measurements.

Reaction of commercially available 3-ethyl-2,4-dimethyl-1*H*-pyrrole with **1** in CH_2Cl_2 containing trifluoroacetic acid, followed by in situ oxidation and chelation with BF_2, produced **2** in 50% yield after extensive column chromatography. A similar procedure, but using 4-bromobenzaldehyde, afforded **3** in modest yield. Removal of the benzyl protecting group under reducing conditions afforded BD-HQ in near quantitative yield. Although this product was isolated and purified, it was found that the crude product after hydrogenation could be taken through to the quinone derivative, BD-Q, by oxidation with DDQ. The isolated yield after purification was a respectable 82%. Preparation of the phenylene-spaced dyad, BD-PQ, was carried out in a similar manner to that described above but using compound **5**. This latter material was prepared in an excellent 90% yield by Suzuki coupling of **3** with the boronic acid **4**. A full range of structural tools, including mass spectrometry, ^1H, ^{13}C, ^{19}F and ^{11}B NMR spectroscopy, elemental analysis, and X-ray crystallography, was used to identify and to confirm purity of the hydroquinone and quinone derivatives.

Crystal Structure Determination

Several of the BODIPY derivatives crystallised to afford X-ray diffraction quality samples. Structures were obtained for **5** (which has three independent molecules in the asymmetric unit), BD-Q, BD-PQ, the dimethoxy derivative of BD-PHQ, and the parent BODIPY with no *meso* substituent, which serves as a reference structure for comparisons. An exhaustive description of each compound is not pre-

sented here, but full details for each structure are given in the Supporting Information. The most interesting structure, especially with regard to the ^{19}F NMR spectrum discussed below, is that of BD-Q as depicted in Figure 1. The molecular geometry clearly shows the relative positioning of the two quinone oxygen atoms with respect to the fluorine atoms attached at the boron centre. The quinone ring is exactly perpendicular to the BODIPY fused ring system (dihedral angle: 90°). The two intramolecular O···F distances are 5.572 Å and 8.094 Å on the two sides of the BODIPY plane. Even the shortest distance is well outside the range expected to yield appreciable lone-pair:lone-pair repulsion between oxygen and fluorine atoms. The two molecules in the unit cell pack in a slightly offset head-to-tail centrosymmetric arrangement. This motif is a common feature for BODIPY derivatives.[26] The shortest intermolecular O···F distance is 3.837 Å.

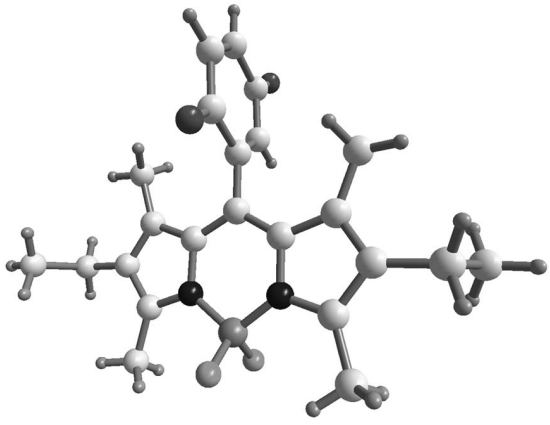

Figure 1. Molecular structure of the quinone derivative BD-Q.

^{19}F NMR Spectroscopy

The most noteworthy NMR spectroscopic finding relates to the ^{19}F spectrum for BD-Q in $CDCl_3$. In all reported literature references, the ^{19}F NMR spectrum corresponds to a single quartet (coupling to ^{11}B: $I = 3/2$, $J \approx 32$ Hz).[27] Indeed, this pattern was seen for the corresponding spectrum of BD-PQ. In the case of BD-Q, however, the ^{19}F NMR spectrum comprises two distinct sets of resonances that after deconvolution contain 8 lines (Figure 2). The entire set of signals could be simulated as an approximate doublet of quartets using J (^{11}B-^{19}F) = 33.5 Hz, J (^{11}B-^{19}F) = 31.0 Hz and J (^{19}F-^{19}F) = 108.7 Hz (see Supporting Information). Evidently, this finding is consistent with each fluorine atom residing in two distinctly different environments. Moreover, the two fluorine atoms (F_a, F_b) can be inequivalent only if rotation of the quinone unit is slow on the NMR time-scale. To explore the possible rotation dynamics, ^{19}F NMR spectra were recorded for BD-Q in [D_8]toluene at temperatures ranging from 303 to 378 K (Supporting Information). At room temperature, the spectrum is similar to that shown in Figure 2, but there is some overlap of signals and satellite peaks from additional coupling to ^{10}B. As the temperature is raised, the resonances show no obvious sign of broadening or coalescence. It would appear that free rotation of the benzene ring is restricted, presumably by the two proximal methyl groups of the BODIPY unit. This finding agrees with molecular dynamics simulations in a solvent matrix that support a severe "rocking" of the ring but without full rotation.

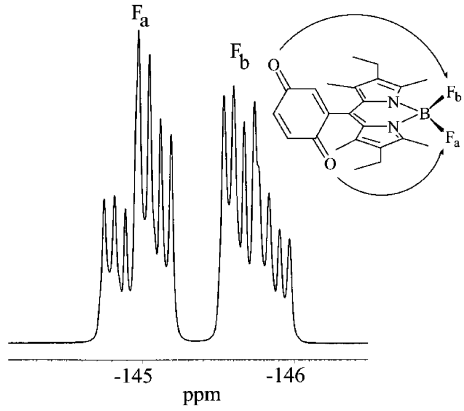

Figure 2. ^{19}F NMR spectrum recorded for BD-Q in $CDCl_3$ showing the coupling patterns and tentative assignment.

Assuming the measured chemical shift for BD-PQ (–145.55 ppm) represents an unperturbed fluorine atom, the more positive chemical shift pattern (–144.97 ppm) must be associated with F_a (Figure 2). It is known that, because of the large polarizability of C–F bonds, ^{19}F chemical shifts are susceptible to weak long-range electronic interactions.[28] Apparently, this is even more so for the B–F bond, presumably because of the increased electronegativity difference between the two atoms. As far as we are aware, splitting of the fluorine resonances has not been reported previously. To see if the phenomenon is unique to the quinone derivative, the ^{19}F NMR spectrum for BD-M was collected under identical conditions. The ^{19}F NMR spectrum (see Supporting Information) is very similar in appearance to that shown in Figure 2. There are, however, subtle differences in the chemical shifts for the two fluorine signals, which suggest that the hydridisation state of oxygen has an effect on the extent of shielding.

Electrochemical Investigations

A full investigation, where possible, of the redox behaviour for the quinone, hydroquinone and dimethoxy derivatives was carried out in CH_2Cl_2 (0.2 M TBATFB) by cyclic voltammetry. Because of solubility problems, the cyclic voltammogram for BD-PHQ was obtained from a solution in dry DMSO. A representative cyclic voltammogram for BD-PQ is presented in the Supporting Information and can be interpreted in terms of the known electrochemical behaviour of isolated BODIPY[29] and quinone derivatives.[30] In each case, one-electron oxidation of BODIPY and one-electron reduction of the quinone correspond to quasi-revers-

ible processes. Collected in Table 1 are the associated half-wave potentials ($E_{1/2}$), vs. Fc^+/Fc, for the various oxidation and reduction processes. There are some important points to note regarding the electrochemical data, especially when comparing the two quinones.

Table 1. Electrochemical data recorded for several of the BODIPY derivatives as defined in the text.

Cmpd.[a]	E_1 [V][b]	E_2 [V][c]	E_3 [V][d]	E_4 [V][e]	ΔE [V][f]
BD-M	–	–1.76	0.61	–	2.37
BD-HQ	–	–1.58	0.82	0.61	2.40
BD-Q	–0.79	–1.81[g]	0.71	–	2.52
BD-PM	–	–1.65	0.73	–	2.38
BD-PHQ[h]	–	–1.50	0.76 [g]	0.56[g]	2.26
BD-PQ	–0.90	–1.79	0.63	–	2.42

[a] In dry CH_2Cl_2 containing 0.2 M TBATFB at Pt electrode, 50 mV s^{-1} scan rate, E values verses Fc^+/Fc ($E_{1/2}$ = 0.44 V). [b] $E_{1/2}$ For one-electron reduction of quinone. [c] $E_{1/2}$ For one-electron reduction of BODIPY. [d] $E_{1/2}$ For one-electron oxidation of BODIPY. [e] $E_{1/2}$ For one-electron oxidation of hydroquinone. [f] $E_3 - E_2$. [g] No reverse peak observed. [h] In DMSO.

Evidently, the ease of reduction and oxidation of the BODIPY core is dependent on the redox state of the appended group. For both sets of dyad, oxidation and reduction is more difficult for the quinone form than for the hydroquinone derivative. Comparison of BD-Q with BD-PQ reveals that reduction of the quinone unit is markedly easier when the unit is attached directly. The corollary is that removal of an electron from the BODIPY unit is made more difficult. However, the difference $E_3 - E_1$ (see Table 1 for description of peak identities) is relatively constant at ca. 1.5 eV for the two compounds.

Photophysical Studies

Photophysical data, including absorption and fluorescence maxima, were collected for all compounds in dry CH_3CN, this being the most suitable solvent to dissolve the hydroquinone derivatives. For comparative purposes, similar data were recorded for the literature compound, BD-P,[31] containing a phenyl group attached to the *meso* position of the BODIPY. As a typical example, a set of absorption/fluorescence profiles for BD-M are shown in Figure 3 and the remaining absorption spectra are given in the Supporting Information. Collected in Table 2 are associated photophysical parameters for the BODIPY derivatives. The lowest-energy energy maximum (λ_{ABS}) for BD-M seen at 521 nm is assigned to the S_0–S_1 electronic transition associated with the BODIPY core. The high molar absorption coefficient (ε_{max}) is in keeping with previous findings.[32] The significantly broader and less intense band seen at ca 380 nm corresponds to the S_0–S_2 transition. The high-energy absorption band can be attributed to π–π* transitions for the appended dimethoxybenzene unit.

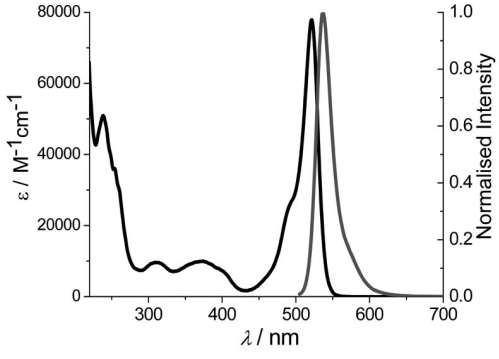

Figure 3. Typical absorption (black) and fluorescence (grey) spectra for BD-M in CH_3CN at room temperature.

Table 2. Collection of photophysical parameters for the series of BODIPY derivatives in CH_3CN at room temperature.

Compound[a]	λ_{ABS} [nm]	λ_{EM} [nm]	ε_{max} (M^{-1} cm^{-1}]	$\Delta\nu_{St}$ [cm^{-1}]	ϕ_{FLU}	τ_{FLU} [ns]	k_{RAD} [$\times 10^8$ s^{-1}]
BD-P[b]	521	535	75300	503	0.67	5.8	1.16
BD-M	523	537	87400	499	0.68	6.0	1.13
BD-HQ	525	539	79400	495	0.05	0.48	1.04
BD-Q	529	547	59700	623	[c]	<0.05	–
BD-PM	521	537	77800	573	0.61	5.6	1.09
BD-PHQ	521	537	78300	573	0.54	5.0	1.08
BD-PQ	523	539	68500	568	[c]	<0.05	–

[a] Abbreviations described in the text. [b] Reference compound is *meso*-phenyldifluoroborondipyrromethene. [c] Too small to be measured accurately.

Room-temperature fluorescence from BD-M is detected readily in fluid solution, the band shape being a good mirror image of the absorption profile. There is also a good match between the excitation and absorption spectra. The small Stokes' shift ($\Delta\nu_{St}$) is in line with previous work on BODIPY compounds and supports the concept of a modest structural change accompanying excitation.[33] The fluorescence quantum yield (ϕ_{FLU}) is comparable to that determined for BD-P under identical conditions, as is the fluorescence lifetime (τ_{FLU}) determined by single-photon counting methods. The decay curve was mono-exponential. The radiative rate constant ($k_{RAD} = \phi_{FLU}/\tau_{FLU}$) remains comparable to literature values. Overall, the methoxy group has little, if any, effect on the photophysical behaviour of the BODIPY dye. Inserting a benzene ring between dye and appended dimethoxybenzene unit has no significant effect on the measured photophysical properties (Table 2).

Conversion of the dimethoxybenzene group into the analogous hydroquinone derivative has little effect on the shape or position of the absorption and fluorescence maxima. Even subjecting the spectral profiles to detailed curve-fitting routines failed to detect significant electronic coupling between the subunits. Furthermore, the Stokes' shifts remain highly comparable to those derived for the reference compounds. There are, however, small perturbations of the measured emission quantum yields and lifetimes consistent with quenching of the S_1 state localised on the BODIPY unit by the appended hydroquinone. On the basis of the electrochemical results, quenching can be attributed to intramolecular electron transfer from the hydroquinone to the excited state of the BODIPY dye, for which the rate constant (k_{ET}) can be determined from Equation (1). Here, τ_{COMP} and τ_{REF} refer to the fluorescence lifetimes of the

compound and its appropriate reference, respectively. The derived k_{ET} values are markedly different for the two derivatives, despite the comparable thermodynamic driving forces (ΔG^0) for light-induced electron transfer. These latter values were estimated from the peak potentials observed in the cyclic voltammograms and corrected for changes in electrostatic potential caused by charge separation.[34] There is only a small driving force for electron transfer, with ΔG^0 changing from –0.09 eV for DB-PHQ to only 0.03 eV for DB-HQ. Nonetheless, k_{ET} for DB-HQ has a value of 1.9×10^9 s^{-1}, which is relatively high and accounts for some 92% of the total deactivation steps. The almost 100-fold increase in k_{ET} found for the directly linked analogue can be ascribed to the shorter separation distance between the redox units.

$$k_{ET} = \left(\frac{1}{\tau_{COMP}} - \frac{1}{\tau_{ref}}\right) \quad (1)$$

The absorption profile, including half-widths, found for BD-PQ is rather similar to that recorded for the control compound but the small red shift and reduced oscillator strength noted for BD-PQ suggests weak electronic interaction between the subunits in this case (Table 2). Extremely weak fluorescence could be detected for BD-Q and BD-PQ at ambient temperature. Time-resolved fluorescence decay profiles were dual exponential, comprising a long-lived component that matched the lifetime of the hydroquinone derivative and an extremely short-lived component with a lifetime that could not be properly resolved from the instrumental response time (ca. 50 ps). The contribution of the longer lifetime component could be reduced, but not completely eradicated, by repeated purification of the samples by preparative TLC. These findings are consistent with minor contamination of the quinone derivatives with their corresponding hydroquinone forms. Hence, it was not possible to measure accurately ϕ_{FLU} values. However, assuming that k_{RAD} remains constant for the BODIPY derivatives, an upper limit for the ϕ_{FLU} of the quinone derivatives is 0.005.

Fluorescence quenching by quinone moieties is well known and can be attributed to light-induced electron transfer.[35a,35b] From the cited electrochemical data (Table 1), ΔG^0 values of –0.90 and –0.83 eV, respectively, can be calculated for BD-Q and BD-PQ. These driving forces are sufficiently large to ensure that oxidative electron transfer competes effectively with the radiative event. In this case, the observed emission yield is set by the level of hydroquinone impurities remaining in the sample. Although we might expect k_{ET} to be much higher for the directly linked analogue than for the phenylene-spaced derivative, this situation is not apparent from the results presented here. Instead, we can only set the lower limit for k_{ET} as being $>2 \times 10^{10}$ s^{-1}. It is evident when comparing BD-HQ and BD-Q, however, that there is not a major on/off fluorescence modulation between the two forms. Thus, for sensing applications, this pair of compounds is rather limited. This is not the case for the phenylene-spaced analogues, where there is a large disparity in emission probabilities for the two forms. The upshot of this finding is that, whereas BD-PQ is non-luminescent, the counterpart, BD-PHQ, displays appreciable fluorescence in fluid solution at room temperature. Thus, the molecules exhibit the on/off luminescence switching required for sensing applications. The external trigger need only serve to interconvert the quinone and hydroquinone moieties.

Spectroelectrochemical and Chemical Fluorescence Switching

Having identified the leading candidates for sensing applications, the next stage involved testing the dyads under rigorously controlled switching conditions. The first set of experiments involved electrochemical modification of the appended quinone group within BD-PQ, using a standard OTTLE cell set-up and controlled fixed-potential electrolysis. The change in fluorescence intensity was monitored over time following reduction of BD-PQ in DCM (0.2 M TBATFB) at –0.9 V vs. Fc/Fc$^+$. At this reduction potential, by inspection of the redox data given in Table 1, we expect to perform one-electron reduction so as to produce the so-called semiquinone (i.e., Q + e$^-$ → Q$^{\cdot-}$). Illustrated in Figure 4 are the corresponding alterations in fluorescence profiles, following electrolysis over some 10 min. After this time there was a noticeable levelling off in fluorescence intensity, which was taken to indicate complete turnover of BD-PQ. By switching the potential of the working electrode to +0.50 V vs. Fc/Fc+, the reverse process could be observed in which fluorescence intensities decreased over time (Supporting Information). This cycle could be repeated many times, without any real drop in performance of the system. To interpret the above observations it is worth noting that the experiments were carried out in a low-polarity aprotic solvent, which simplifies somewhat electrochemical processes regarding quinones; no protonated forms need to be considered.[36] The exhaustive reductive electrolysis presumably builds up the concentration of semiquinone at the working electrode, which is known to disproportionate to the dianion (2Q$^{\cdot-}$ → Q^{2-} + Q). The dianion, being a poor quencher, leads to the observed fluorescence change.

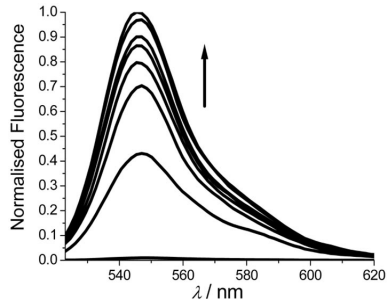

Figure 4. Observed increase in fluorescence intensity upon fixed-potential reduction of BD-PQ ($c \approx 4$ μM) in DCM (0.2 M TBATFB) using a conventional OTTLE cell.

Because lipid oxidative stress is a well established cause of cell damage,[37] we were interested to test the reporting capabilities of the two redox sensors in a lipid-like environment. To mimic lipid membranes, micelles dispersed in water have been used widely,[38] seeing as they can encapsulate organic molecules in the hydrophobic core. The two compounds, BD-PQ and BD-PHQ, are totally insoluble in water. However, careful sonication of a few milligrams of each compound in water containing 5% v/v Triton-X and filtering afforded noticeably coloured solutions. The absorption spectra recorded at 25 °C for separate solutions of BD-PQ and BD-PHQ (Supporting Information) displayed the characteristic profiles seen previously (Figure 3). Moreover, the narrow band-shapes support lack of any appreciable self-aggregation of the compounds within the micelles. The concentration of the two solutions, assuming that ε_{max} values do not change widely, are similar and around 4 μM. An especially prevalent ROS is peroxide, and so to test its possible detection, sodium percarbonate was added to the micelle solution containing BD-PHQ (4 μM) and Na_2HPO_4 (0.18 M). We considered that under these conditions the H_2O_2 released by the percarbonate would oxidise the hydroquinone to quinone, and thus bring about efficient fluorescence modulation. The dramatic reduction in recorded fluorescence emission (Figure 5) over some 10 min after peroxide formation is fully consistent with the formation of BD-PQ by the proposed chemical transformation. Under control conditions without percarbonate, no change in emission signal was noted. It was especially encouraging that a very clear-cut difference in on/off signal was readily observable to the naked eye, as shown in the insert of Figure 5.

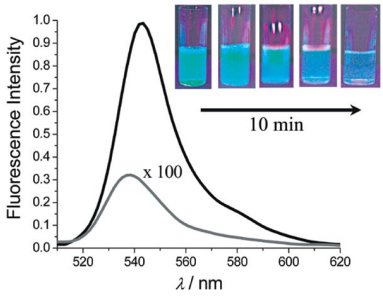

Figure 5. Fluorescence spectra recorded at 25 °C for BD-PHQ ($c \approx 4$ μM) in distilled water containing Triton-X (5% v/v) and Na_2HPO_4 (0.18 M), before (dark line) and after (grey line) the addition of $Na_2CO_3.H_2O_2$. Excitation wavelength λ = 495 nm. Insert shows a cuvette illuminated with a standard UV-lamp, and the changes in fluorescence over time during oxidation by peroxide.

To assess the reversibility of the process, the BD-PQ (4 μM) solution was treated with sodium ascorbate (1.1 M). The tenet here is that ascorbate would gradually reduce the quinone unit and thus switch on fluorescence. Indeed, we observed a recovery of the fluorescence signal fully consistent with the generation of BD-PHQ (see Supporting Information). More encouragingly, control experiments carried out on BD-P under similar conditions to the above (Supporting Information) showed only modest fluorescence alterations. We expected some oxidation of the BODIPY unit by peroxide, which is observed, but the change in fluorescence signal is only ca. 30% over 10 min. By comparison, under reducing conditions with ascorbate the change is fluorescence intensity is only ca. 10%. These two competing redox reactions presumably take place for BD-PQ and BD-P, but are much slower than the redox processes at the quinone/hydroquinone moieties. This seems reasonable considering the disparate redox potentials between, for example, the quinone and BODIPY subunits (Table 1). Overall, chemically induced, reversible cycling of the redox couple looks entirely feasible.

Conclusions

By precise positioning of a redox-active unit on the highly fluorescent BODIPY scaffold it has been possible to produce an extremely responsive on/off fluorescent molecular probe. Although many different fluorophores have found applications in the sensing field, the BODIPY unit is emerging as a frontrunner.[39] In fact, the number of BODIPY-based derivatives for applications as probes in the sensing field, toward species such as cations (i.e., Zn^{2+}, K^+, Hg^{2+}, Cd^{2+}),[40–43] gases (O_2, NO)[44,45a,45b] and thiols,[46] is growing constantly. It is worth noting that use of BODIPY-based molecules for detection of ROS and monitoring lipid oxidation in living cells have been developed.[47–50] The technique, however, relies on ratio-imaging and the loss of fluorescence caused by direct oxidation of the dye. This method has the clear disadvantage that the chromophore is destroyed. A more recyclable system is feasible using our outlined method, but clearly more testing is required using different ROS, to evaluate parameters such as selectivity, compound degradation and biocompatibility. We expect to address these factors at a later date.

Experimental Section

General: Solvents were dried by standard literature methods before being distilled and stored under nitrogen over 4-Å molecular sieves.[51] ^1H and ^{13}C NMR spectra were recorded with either a Bruker AVANCE 300 MHz or a JEOL Lambda 500 MHz spectrometers. Chemical shifts for ^1H and ^{13}C NMR spectra are referenced relative to the residual protiated solvent. The ^{11}B NMR chemical shift is referenced relative to $BF_3{\cdot}Et_2O$ (δ = 0 ppm), and the ^{19}F NMR chemical shift is given relative to $CFCl_3$ (δ = 0 ppm). The ^{19}F NMR spectrum for BD-Q was simulated using the program NUMARIT. To simplify the calculation, the fluorine couplings to ^{10}B (I = 3) were ignored because of its low relative abundance. Routine mass spectra were obtained using in-house facilities and elemental analysis was performed at Medac Ltd. Commercial starting materials, 4-bromobenzaldehyde, 2,5-dihydroxybenzaldehye, 3-ethyl-2,4-dimethyl-1*H*-pyrrole and 2-bromophenyl-1,4-diol, were used as received. Compound **1** was made by the literature procedure.[52]

Absorption spectra were recorded with a Hitachi U3310 spectrophotometer while fluorescence studies were made with a Hitachi F-4500 fluorescence spectrophotometer. Fluorescence spectra were

corrected for spectral imperfections using a standard lamp. Measurements were made using optically dilute solutions after deoxygenation by purging with dried N_2. Fluorescence quantum yields were measured with respect to BD-P (Φ_F = 0.67, MeCN).[53] Corrected excitation spectra were also recorded under optically dilute conditions. Fluorescence lifetimes were measured by time-correlated, single-photon counting following excitation with an ultrashort laser diode emitting at 525 nm using a PTI Easylife spectrometer. After deconvolution of the instrumental response function, the temporal resolution of this set-up was ca. 50 ps.

Cyclic voltammetry experiments were performed using a fully automated HCH Instruments Electrochemical Analyzer and a three-electrode set-up consisting of a platinum working electrode, a platinum wire counter electrode and a silver wire reference electrode. Ferrocene was used as an internal standard. All studies were performed in deoxygenated DCM or DMSO containing tetra-*N*-butylammonium tetrafluoroborate (TBATFB) (0.2 M) as background electrolyte. The solute concentrations were typically 0.5 mM. Redox potentials were reproducible to within ±15 mV. Spectroelectrochemical fluorescence experiments were performed using a Specac Ominicell, which was aligned 45° to the excitation source and illuminated at 495 nm. Scattered and incident light was removed using a filter placed before the detector. Fluorescence spectra were imported into the commercial package Origin, baseline corrected and smoothed. Control experiments, to determine any possible quenching effects of background electrolyte, were carried out by measuring ϕ_{FLU} and λ_{EM} for equimolar solutions of BD-PQ in DCM in the presence and absence of 0.2 M TBATFB; no appreciable changes were observed.

Preparation of 4: Benzyl bromide (1.51 mL, 12 mmol, 2.4 equiv.) was added to a stirred solution of 2-bromo-1,4-dihydroxybenzene (1 g, 5.29 mmol, 1 equiv.) and K_2CO_3 (1.02 g, 7.41 mmol, 1.4 equiv.) in acetone (25 mL). The resulting mixture was heated to reflux until TLC showed complete consumption of the aldehyde. The reaction mixture was cooled, and the potassium carbonate was separated via filtration. The reaction solvent was removed under reduced pressure to yield a grey solid, which was taken up into DCM (100 mL) and washed with water (100 mL). The organic layer was separated, dried ($MgSO_4$) and removed to yield the crude product. This was purified on silica gel using petroleum ether/ethyl acetate (4:1) to afford the product as a white solid (1.76 g, 91%); m.p. 47–49 °C. ^{1}H NMR ($CDCl_3$, 300 MHz): δ = 7.40 (m, 10 H), 7.25 (dd, J = 2.4, J' = 0.6 Hz), 6.86 (m, 2 H), 5.09 (s, 2 H), 5.00 (s, 2 H) ppm.

*t*BuLi (1.7 M, 4.01 mL, 6.82 mmol, 1.4 equiv.) was added dropwise to a stirred solution of the above material (1.8 g, 4.87 mmol, 1 equiv.) in THF (50 mL) at –78 °C, immediately followed by the dropwise addition of triethyl borate (2.48 mL, 14.6 mmol, 3 equiv.) at –78 °C. This temperature was maintained for 10 min, after which the solution was warmed to room temperature and stirred for 2 h. The reaction was cooled to 0 °C and quenched with a saturated solution of ammonium chloride (30 mL), followed by removal of the solvent under reduced pressure. The residue was extracted with ethyl acetate (3 × 100 mL), which was washed with water (100 mL) and brine (100 mL). The organic layer was separated, dried ($MgSO_4$), and the solvent removed under reduced pressure to yield the crude product. This was purified on silica gel using petroleum ether/ethyl acetate (3:2) as eluant to afford the product as a white solid (1.3 g, 83% yield); m.p. 113–115 °C. ^{1}H NMR ($CDCl_3$, 300 MHz): δ = 7.55 (d, J = 3.1 Hz, 1 H), 7.39 (m, 10 H), 7.05 (dd, J = 8.9, J' = 3.1 Hz, 1 H), 6.92 (d, J = 8.9 Hz, 1 H), 6.49 (br. s, 2 H), 5.10 (s, 2 H), 5.07 (s, 2 H) ppm. ^{13}C NMR ($CDCl_3$, 75 MHz): δ = 158.82, 153.89, 137.82, 136.73, 129.24, 128.84, 128.17, 128.06, 127.83, 122.95, 120.07, 113.34, 71.99, 71.26 ppm. IR (neat): $\tilde{\nu}$ = 3494, 3389 (O–H), 2875 (C–H) cm^{-1}.

Preparation of 2: TFA (8 drops) was added dropwise to a stirred solution of 3-ethyl-2,4-dimethyl-1*H*-pyrrole (2.16 mL, 16 mmol, 1 equiv.) and 2,5-dibenzyloxybenzaldehyde (2.55 g, 8 mmol, 0.5 equiv.) in DCM (600 mL). The reaction was stirred at room temperature until TLC showed complete consumption of the aldehyde. DDQ (1.82 g, 8 mmol, 0.5 equiv.) was added in a single portion, and the reaction was stirred at room temperature overnight. *N*,*N*-Diisopropylethylamine (15.88 mL, 91 mmol, 5.7 equiv.) and $BF_3{\cdot}Et_2O$ (16.22 mL, 128 mmol, 8 equiv.) were added, and the reaction was stirred at room temperature for 6 h. The reaction mixture was washed with water (3 × 100 mL) and brine (3 × 100 mL). The separated organic fractions were dried ($MgSO_4$), filtered and the solvent removed to yield a black/dark-violet residue with a green tint. The residue was chromatographed on silica gel using toluene eluant to afford a red solid (2.38 g, 50% yield); m.p. 53–55 °C. ^{1}H NMR ($CDCl_3$, 300 MHz): δ = 7.35 (m, 10 H), 7.08 (dd, J = 8.9, J' = 2.9 Hz, 1 H), 7.02 (d, J = 8.9 Hz, 1 H), 6.88 (d, J = 2.9 Hz, 1 H), 5.11 (s, 4 H), 2.63 (s, 6 H), 2.38 (q, J = 7.5 Hz, 4 H), 1.39 (s, 6 H), 1.11 (t, J = 7.5 Hz, 6 H) ppm. ^{13}C NMR ($CDCl_3$, 75 MHz): δ = 152.31, 151.85, 148.81, 136.34, 135.79, 135.49, 135.34, 130.89, 129.43, 126.92, 126.74, 126.28, 126.04, 125.78, 125.39, 124.97, 115.86, 115.39, 113.80, 69.66, 69.46, 15.49, 12.83, 10.81, 9.49 ppm. IR (neat): $\tilde{\nu}$ = 2962, 2928, 2869 (C–H), 1539, 1475 (C=C, C=N), 1187 (B–F) cm^{-1}. MS (EI): m/z = 592 [M]$^+$. $C_{37}H_{39}BF_2N_2O_2$ (592): calcd. C 75.00, H 6.63, N 4.73; found C 74.88, H 6.72, N 4.59.

Preparation of 3: TFA (8 drops) was added dropwise to a stirred solution of 3-ethyl-2,4-dimethyl-1*H*-pyrrole (2.16 mL, 16 mmol, 1 equiv.) and 4-bromobenzaldehyde (1.48 g, 8 mmol, 0.5 equiv.) in DCM (600 mL). The reaction was stirred at room temperature until TLC showed complete consumption of the aldehyde. DDQ (1.82 g, 8 mmol, 0.5 equiv.) was added in a single portion, and the reaction was stirred at room temperature overnight. *N*,*N*-Diisopropylethylamine (15.88 mL, 91 mmol, 5.7 equiv.) and $BF_3{\cdot}Et_2O$ (16.22 mL, 128 mmol, 8 equiv.) were added, and the reaction was stirred at room temperature for 6 h. The reaction mixture was washed with water (3 × 100 mL) and brine (3 × 100 mL). The separated organic fractions were dried ($MgSO_4$), filtered and the solvent removed to yield a black/dark-violet residue with a green tint. The residue was chromatographed on silica gel using toluene eluant to afford a dark red/purple solid (1.73 g, 47% yield); m.p. 240–242 °C. ^{1}H NMR ($CDCl_3$, 300 MHz): δ = 7.64 (d, J = 8.3 Hz, 2 H), 7.18 (d, J = 8.3 Hz, 2 H), 2.532 (s, 6 H), 2.31 (q, J = 7.5 Hz, 4 H), 1.32 (s, 6 H), 0.98 (t, J = 7.5 Hz, 6 H) ppm. ^{13}C NMR ($CDCl_3$, 75 MHz): δ = 154.65, 138.93, 138.41, 138.15, 135.35, 133.46, 132.63, 131.07, 123.41, 17.39, 14.69, 12.76, 12.16 ppm. MS (EI): m/z = 458 [M]$^+$. $C_{23}H_{26}BBrF_2N_2$ (458): calcd. C 60.16, H 5.71, N 6.10; found C 60.07, H 5.65, N 6.12.

Preparation of 5: The compounds **3** (1.62 g, 3.52 mmol, 1 equiv.) and **4** (1.29 g, 3.87 mmol, 1.1 equiv.) were dissolved in THF (50 mL), and the resulting solution was purged with nitrogen for 1 h. To this solution was added a nitrogen-purged aqueous solution of 2 M Na_2CO_3 (5.5 mL, 11 mmol, 3 equiv.), followed by Pd(PPh_3)$_4$ (0.123 g, 3 mol-%). The reaction mixture was refluxed overnight. The THF was removed under reduced pressure and the residue was taken up into DCM (100 mL), which was washed with brine (2 × 50 mL), separated and dried ($MgSO_4$). After filtration, the solvent was removed under reduced pressure, to yield a dark red residue. The residue was chromatographed on silica gel using

DCM/petroleum ether (1:1) as eluant to afford a light red solid (2.11 g, 90% yield); m.p. 78–80 °C. ^{1}H NMR ($CDCl_3$, 300 MHz): δ = 7.71 (d, J = 8.2 Hz, 2 H), 7.38 (m, 12 H), 7.12 (d, J = 2.9 Hz, 1 H), 7.04 (d, J = 8.9 Hz, 1 H), 6.97 (dd, J = 8.9, J' = 2.9 Hz), 5.11 (s, 2 H), 5.01 (s, 2 H), 2.57 (s, 6 H), 2.33 (q, J = 7.5 Hz, 4 H), 1.36 (s, 6 H), 1.02 (t, J = 7.5 Hz, 6 H) ppm. ^{13}C NMR ($CDCl_3$, 75 MHz): δ = 154.12, 150.76, 140.75, 139.59, 138.79, 137.73, 134.97, 133.14, 132.61, 131.38, 130.51, 128.89, 128.66, 128.40, 128.26, 128.01, 127.83, 127.41, 118.58, 115.96, 115.24, 72.11, 72.44, 17.44, 14.75, 12.75, 12.02 ppm. IR (neat): $\tilde{\nu}$ = 2962, 2869 (C–H), 1538, 1475 (C=C, C=N), 1188 (B–F) cm^{-1}. MS (EI): m/z = 668 [M]$^+$. $C_{43}H_{43}BF_2N_2O_2$ (668): calcd. C 77.24, H 6.48, N 4.19; found C 76.71, H 6.48, N 4.06.

Preparation of BD-PQ: A stirred solution of **5** (1.8 g, 2.69 mmol, 1 equiv.) and Pd/C 10% (0.7 g) in MeOH (50 mL) was subjected to hydrogenation at 4 atm pressure until TLC showed complete consumption of both the starting material and the mono-deprotected intermediate. The reaction mixture was filtered through a pad of Celite to remove the catalyst, and the reaction solvent removed to yield the dihydroxy product, which was crudely purified by washing with petroleum ether. To a stirred solution of the crude product in THF (50 mL) was added DDQ (1.34 g, 5.91 mmol, 2.2 equiv.). On addition of DDQ the reaction mixture changed colour from red to dark purple. When TLC showed complete consumption of the dihydroxy crude product, the reaction solvent was removed and the remaining residue was taken into DCM (50 mL), washed with water, and the combined organic fractions were dried ($MgSO_4$). The solvent was removed under reduced pressure, yielding a purple crude product, which was purified on a silica gel using chloroform as eluant, followed by washing with petroleum ether, to afford the purple product (1.09 g, 83% yield); m.p. >290 °C. ^{1}H NMR ($CDCl_3$, 300 MHz): δ = 7.65 (d, J = 8.3 Hz, 2 H), 7.39 (d, J = 8.3 Hz, 2 H), 6.98 (d, J = 2.2 Hz, 1 H), 6.91 (d, J = 10 Hz, 1 H), 6.86 (dd, J = 10, J' = 2.2 Hz, 1 H), 2.53 (s, 6 H), 2.29 (q, J = 7.5 Hz, 4 H), 1.303 (s, 6 H), 0.98 (t, J = 7.5 Hz, 6 H) ppm. ^{13}C NMR ($CDCl_3$, 75 MHz): δ = 187.46, 186.54, 154.61, 145.49, 139.31, 138.46, 138.33, 137.47, 136.62, 133.71, 133.42, 133.33, 131.01, 130.14, 129.21, 17.39, 14.70, 12.77, 12.09 ppm. ^{11}B NMR ($CDCl_3$, 160 MHz): δ = –0.153 (t, $J_{B\text{-}F}$ = 31.4 Hz) ppm. ^{19}F NMR ($CDCl_3$, 470 MHz): δ = –145.550 (q, $J_{B\text{-}F}$ = 33.1 Hz) ppm. IR (neat): $\tilde{\nu}$ = 2964 (C–H), 1656 (C=O), 1538, 1473 (C=C, C=N), 1183 (B–F) cm^{-1}. MS (EI): m/z = 486 [M]$^+$. $C_{29}H_{29}BF_2N_2O_2$ (486): calcd. C 71.62, H 6.01, N 5.76; found C 71.03, H 5.79, N 5.31.

Analytical Data

BD-PHQ: M.p. >290 °C. ^{1}H NMR ([D$_6$]DMSO, 300 MHz): δ = 8.96 (br. s, 1 H), 8.83 (br. s, 1 H), 7.74 (d, J = 7.9 Hz, 2 H), 7.34 (d, J = 7.9 Hz, 2 H), 6.79 (m, 2 H), 6.63 (dd, J = 8.5, J' = 2.6 Hz, 1 H), 2.44 (s, 6 H), 2.30 (q, J = 7.5 Hz, 4 H), 1.34 (s, 6 H), 0.95 (t, J = 7.5 Hz, 6 H) ppm. ^{13}C NMR ([D$_6$]DMSO, 75 MHz): δ = 153.44, 150.65, 147.31, 141.13, 139.95, 138.55, 133.14, 132.96, 130.61, 129.84, 127.99, 127.58, 117.64, 116.89, 116.00, 16.77, 14.67, 12.52, 11.75 ppm. IR (neat): $\tilde{\nu}$ = 3353, 3522 (O–H), 2964, 2931 (C–H), 1538, 1474 (C=C, C=N), 1186 (B–F) cm^{-1}. MS (EI): m/z = 488 [M]$^+$.

Preparation of BD-Q: A similar procedure was used to that described above. **2** (1 g, 1.69 mmol, 1 equiv.), Pd/C 10% (0.3 g), MeOH (50 mL), DDQ (0.84 g, 3.72 mmol, 2.2 equiv.). Purification: silica gel DCM eluant, petroleum ether wash. Yield 0.57 g, 82%; m.p. 169–171 °C. ^{1}H NMR ($CDCl_3$, 300 MHz): δ = 6.94 (d, J = 10.1 Hz, 1 H), 6.89 (dd, J = 10.9, J' = 2.2 Hz, 1 H), 6.82 (d, J = 2.2 Hz, 1 H), 2.48 (s, 6 H), 2.30 (q, J = 7.5 Hz, 4 H), 1.83 (s, 6 H), 0.97 (t, J = 7.5 Hz, 6 H) ppm. ^{13}C NMR ($CDCl_3$, 75 MHz): δ = 186.19, 185.57, 155.74, 144.66, 137.67, 137.15, 136.62, 136.30, 133.97, 130.64, 129.93, 17.38, 14.68, 13.20, 12.85 ppm. ^{11}B NMR ($CDCl_3$, 160 MHz): δ = –0.343 (t, $J_{B\text{-}F}$ = 33.0 Hz) ppm. ^{19}F NMR ($CDCl_3$, 470 MHz): δ = –144.97 (dq, $J_{F\text{-}F}$ = 102, $J_{B\text{-}F}$ = 32.2 Hz), –145.75 (dq, $J_{F\text{-}F}$ = 102, $J_{B\text{-}F}$ = 30.7 Hz) ppm. IR (neat): $\tilde{\nu}$ = 2964, 2929, 2872 (C–H), 1656 (C=O), 1544, 1474 (C=C, C=N), 1187 (B–F) cm^{-1}. MS (EI): m/z = 410 [M]$^+$. $C_{23}H_{25}BF_2N_2O_2$ (410): calcd. C 67.33, H 6.14, N 6.82; found C 67.16, H 6.17, N 6.69.

Analytical Data

BD-HQ: M.p. >290 °C. ^{1}H NMR (MeOD, 300 MHz): δ = 6.78 (m, 2 H), 6.52 (dd, J = 2.1, J' = 1.2 Hz, 1 H), 2.47 (s, 6 H), 2.36 (q, J = 7.5 Hz, 4 H), 1.54 (s, 6 H), 1.01 (t, J = 7.5 Hz, 6 H) ppm. ^{13}C NMR (MeOD, 75 MHz): δ = 154.68, 153.05, 148.57, 140.21, 139.62, 134.13, 132.70, 124.80, 119.06, 118.75, 117.50, 18.17, 15.22, 12.89, 11.67 ppm. IR (neat): $\tilde{\nu}$ = 3365 (O–H), 2964, 2931, 2872 (C–H), 1545, 1474 (C=C, C=N), 1195 (B–F) cm^{-1}. MS (EI): m/z = 412 [M]$^+$.

BD-M: Prepared by a similar manner to compound **2**. Yield 40%; m.p. 195–196 °C. ^{1}H NMR ($CDCl_3$, 300 MHz): δ = 6.97 (dd, J = 8.9, J' = 2.9 Hz, 1 H), 6.91 (d, J = 8.9 Hz, 1 H), 6.73 (d, J = 2.9 Hz, 1 H), 3.76 (s, 3 H), 3.72 (s, 3 H), 2.53 (s, 6 H), 2.31 (q, J = 7.5 Hz, 4 H), 1.39 (s, 6 H), 0.99 (t, J = 7.5 Hz, 6 H) ppm. ^{13}C NMR ($CDCl_3$, 75 MHz): δ = 155.15, 153.72, 151.38, 138.22, 137.38, 132.77, 131.29, 126.04, 116.06, 115.99, 113.23, 56.57, 56.37, 17.42, 14.78, 12.74, 11.28 ppm. ^{19}F NMR ($CDCl_3$, 470 MHz): δ = –145.356 (dq, $J_{F\text{-}F}$ = 109, $J_{B\text{-}F}$ = 33.8 Hz), –146.085 (dq, $J_{F\text{-}F}$ = 109, $J_{B\text{-}F}$ = 32.3 Hz) ppm. MS (EI): m/z = 440 [M]$^+$.

BD-PM: Prepared by a similar manner to compound **5**. Yield 90%; m.p. 140–142 °C. ^{1}H NMR ($CDCl_3$, 300 MHz): δ = 7.67 (d, J = 8.3 Hz, 2 H), 7.30 (d, J = 8.3 Hz, 2 H), 6.96 (m, 2 H), 6.88 (dd, J = 8.9, J' = 2.9 Hz, 1 H), 3.84 (s, 3 H), 3.76 (s, 3 H), 2.54 (s, 6 H), 2.31 (q, J = 7.5 Hz, 4 H), 1.37 (s, 6 H), 0.99 (t, J = 7.5 Hz, 6 H) ppm. ^{13}C NMR ($CDCl_3$, 75 MHz): δ = 154.70, 154.05, 151.61, 140.78, 139.54, 138.80, 134.84, 133.11, 131.82, 131.36, 130.30, 128.36, 117.27, 114.55, 114.07, 57.22, 56.26, 17.43, 14.76, 12.75, 12.04 ppm. ^{11}B NMR ($CDCl_3$, 160 MHz): δ = –0.106 (t, $J_{B\text{-}F}$ = 31.9 Hz) ppm. ^{19}F NMR ($CDCl_3$, 470 MHz): δ = –145.587 (q, $J_{B\text{–}F}$ = 31.7 Hz) ppm. MS (EI): m/z = 516 [M]$^+$.

Supporting Information (see also the footnote on the first page of this article): Additional cyclic voltammetry results, X-ray crystallographic data, NMR spectra and absorption/fluorescence spectra.

Acknowledgments

This work was supported by Newcastle University and the Engineering and Physical Sciences Research Council (EPSRC)(EP/D032946/1). We thank the EPSRC Mass Spectromery Service at Swansea for obtaining mass spectra. Prof. William McFarlane is thanked for collecting the ^{11}B and ^{19}F NMR spectra, while Dr Bruce Tattershall is thanked for help in simulation of the ^{19}F NMR spectroscopic data.

[1] W. Tan, R. Kopelman, *Handbook of Nanostructured Materials and Nanotechnology* (Ed.: H. S. Nalwa), Academic Press, **2000**, 4, pp. 621–667.
[2] D. W. M. Arrigan, *Analyst* **2004**, *129*, 1157–1165.
[3] P. Ugo, L. M. Moretto, F. Vezzà, *ChemPhysChem* **2002**, *3*, 917–925.
[4] A. Nazarov, D. Thierry, *Electrochim. Acta* **2004**, *49*, 2717–2724.
[5] G. Liu, Y. Lin, Y. Tu, Z. Ren, *Analyst* **2005**, *130*, 1098–1101.
[6] B. Bourlon, J. Wong, C. Miko, L. Forro, M. Bockrath, *Nature Nanotechnol.* **2007**, *2*, 104–107.

[7] L. Basabe-Desmonts, D. N. Reinhoudt, M. Crego-Calama, *Chem. Soc. Rev.* **2007**, *36*, 993–1017.
[8] A. C. Benniston, A. Harriman, I. Llarena, C. A. Sams, *Chem. Mater.* **2007**, *19*, 1931–1938.
[9] S. M. Nie, R. N. Zare, *Ann. Rev. Biophys. Biomol. Struct.* **1997**, *26*, 567–596.
[10] C. Piguet, *Chimia* **1996**, *50*, 144–153.
[11] A. C. Benniston, A. Harriman, S. L. Howell, C. A. Sams, Y.-G. Zhi, *Chem. Eur. J.* **2007**, *13*, 4665–4674.
[12] P. J. Jiang, Z. J. Guo, *Coord. Chem. Rev.* **2004**, *248*, 205–229.
[13] L. Fabbrizzi, A. Poggi, *Chem. Soc. Rev.* **1995**, *24*, 197–202.
[14] K. Rurack, U. Resch-Genger, *Chem. Soc. Rev.* **2002**, *31*, 116–127.
[15] X. M. Gao, Y. L. Zhang, B. H. Wang, *New J. Chem.* **2005**, *29*, 579–586.
[16] T. W. Bell, N. M. Hext, *Chem. Rev.* **2004**, *33*, 589–598.
[17] E. G. Matveeva, G. Shan, I. M. Kennedy, S. J. Gee, D. W. Stoutamire, B. D. Hammock, *Anal. Chim. Acta* **2001**, *444*, 103–117.
[18] G. Y. Ma, Q. Cheng, *Langmuir* **2006**, *22*, 6743–6745.
[19] S. Bencic-Nagale, T. Sternfeld, D. R. Walt, *J. Am. Chem. Soc.* **2006**, *128*, 5041–5048.
[20] a) B. Heyne, V. Maurel, J. C. Sciano, *Org. Biomol. Chem.* **2006**, *4*, 802–807; b) B. Heyne, C. Beddie, J. C. Sciano, *Org. Biomol. Chem.* **2007**, *5*, 1454–1458.
[21] A. Gomes, E. Fernandes, J. L. F. C. Lima, *J. Biochem. Bioph. Methods* **2005**, *65*, 45–80.
[22] a) V. Goulle, A. Harriman, J.-M. Lehn, *J. Chem. Soc., Chem. Commun.* **1993**, 1034–1036; b) A. C. Benniston, G. Chapman, A. Harriman, S. A. Rostron, *Inorg. Chem.* **2005**, *44*, 4029–4036.
[23] a) T. Ueno, Y. Uano, H. Kojima, T. Nagano, *J. Am. Chem. Soc.* **2006**, *128*, 10640–10641; b) A. Harriman, L. J. Mallon, G. Ulrich, R. Ziessel, *ChemPhysChem* **2007**, *8*, 1207–1214.
[24] K. Kayanasundaram, *Coord. Chem. Rev.* **1982**, *46*, 159–244.
[25] G. Ulrich, R. Ziessel, A. Harriman, *Angew. Chem. Int. Ed.* **2008**, *47*, 1184–1201.
[26] B. Herradón, A. Chana, M. Alonso, F. Amat-Guerri, M. Liras, M. A. Maestro, *J. Mol. Struct.* **2004**, *697*, 29–40.
[27] R. Ziessel, L. Bonardi, G. Ulrich, *Dalton Trans.* **2006**, 2913–2918.
[28] J. G. Pearson, E. Oldfield, F. S. Lee, A. Warshel, *J. Am. Chem. Soc.* **1993**, *115*, 6851–6862.
[29] R. Ziessel, C. Goze, G. Ulrich, M. Céario, P. Retailleau, A. Harriman, J. P. Rostron, *Chem. Eur. J.* **2005**, *11*, 7366–7378.
[30] a) M. Bauscher, W. Mäntele, *J. Phys. Chem.* **1992**, *96*, 11101–11108; b) N. Gupta, H. Linschitz, *J. Am. Chem. Soc.* **1997**, *119*, 6384–6391.
[31] P. Toele, H. Zhang, C. Trieflinger, J. Daub, M. Glasbeek, *Chem. Phys. Lett.* **2003**, *368*, 66–75.
[32] J. Karolin, L. Strandberg, L. B. A. Johansson, *J. Am. Chem. Soc.* **1994**, *116*, 7801–7806.
[33] Z. Shen, H. Röhr, K. Rurack, H. Uno, M. Spieles, B. Shulz, G. Reck, N. Ono, *Chem. Eur. J.* **2004**, *10*, 4853–4871.
[34] H. Yao, R. Okada, N. Matag, *J. Phys. Chem.* **1989**, *93*, 7388–7394.
[35] a) L. R. Khundkar, J. W. Perry, J. E. Hanson, P. B. Dervan, *J. Am. Chem. Soc.* **1994**, *116*, 9700–9709; b) D. Gust, T. A. Moore, *Science* **1989**, *244*, 35–41.
[36] *The Chemistry of the Quinonoid Compounds*, vol. 2 (Eds.: S. Patai, Z. Rappoport) Wiley, **1988**. pp. 719.
[37] T. Káli, E. Hideg, I. Vass, K. Hideg, *Free Radical Biol. Med.* **1998**, *24*, 649–652.
[38] J. Gallay, M. Vincent, C. Nicot, M. Waks, *Biochem.* **1987**, *26*, 5738–5747.
[39] R. Ziessel, G. Ulrich, A. Harriman, *New J. Chem.* **2007**, *31*, 496–501.
[40] Y. Mei, P. A. Bentley, *Bioorg. Med. Chem. Lett.* **2006**, *16*, 3131–3134.
[41] a) J.-P. Malval, I. Leray, B. Valeur, *New J. Chem.* **2005**, *29*, 1089–1094; b) M. Baruah, W. Qin, R. A. L. Vallée, D. Beljonne, T. Rohand, W. Dehaen, N. Boens, *Org. Lett.* **2005**, *7*, 4377–4380.
[42] A. Coskun, M. Deniz Yilmaz, E. U. Akkaya, *Org. Lett.* **2007**, *9*, 607–609.
[43] X. Peng, J. Du, J. Fan, J. Wang, Y. Wu, J. Zhao, S. Sun, T. Xu, *J. Am. Chem. Soc.* **2007**, *129*, 1500–1501.
[44] E. J. Park, K. R. Reid, W. Tang, R. T. Kennedy, R. Kopelman, *J. Mater. Chem.* **2005**, *15*, 2913–2919.
[45] a) X. Zhang, H.-S. Zhang, *Spectrochim. Acta* **2005**, *61*, 1045–1049; b) Y. Gabe, T. Ueno, Y. Urano, H. Kojima, T. Nagano, *Anal. Bioanal. Chem.* **2006**, *386*, 621–626.
[46] T. Matsumoto, Y. Urano, T. Shoda, H. Kojima, T. Nagano, *Org. Lett.* **2007**, *9*, 3375–3377.
[47] E. H. W. Pap, G. P. C. Drummen, V. J. Winter, T. W. A. Kooij, P. Rijken, K. W. A. Wirtz, J. A. F. Op den Kamp, W. J. Hage, J. A. Post, *FEBS Lett.* **1999**, *453*, 278–282.
[48] A. C. Nicolescu, Q. Li, L. Brown, G. R. J. Thatcher, *Nitric Oxide* **2006**, *15*, 163–176.
[49] H. D. Guthrie, G. R. Welch, *J. Anim. Sci.* **2007**, *85*, 1402–1411.
[50] N. Itoh, J. Cao, Z.-H. Chen, Y. Yoshida, E. Niki, *Bioorg. Med. Chem. Lett.* **2007**, *17*, 2059–2063.
[51] W. L. F. Armarego, C. L. L. Chai, *Purification of Laboratory Chemicals*, 5th ed., Butterworth-Heineman, London, **2003**.
[52] F. Mu, E. Hamel, D. J. Lee, D. E. Pryor, M. Cushman, *J. Med. Chem.* **2003**, *46*, 1670–1682.
[53] A. Loudet, K. Burgess, *Chem. Rev.* **2007**, *107*, 4891–4932.

Received: February 18, 2008
Published Online: April 15, 2008

